Evaluation of the feasibility of the powder injection moulding process for the fabrication of nuclear fuel and comparison of several formulations

Julien Bricout, Philippe Matheron, Carine Ablitzer, Jean-Claude Gélin, Méryl Brothier, Thierry Barrière

Evaluation of the feasibility of the powder injection moulding process for the fabrication of nuclear fuel and comparison of several formulations

J. Bricout [a], P. Matheron [a], C. Ablitzer [a,*], J.C. Gelin [b], M. Brothier [a], Th. Barrière [b]

[a] CEA, DEN, DEC, SPUA, LCU, Cadarache, F-13108 Saint-Paul Lez Durance, France
[b] Université de Franche-Comté, FEMTO-ST, 32 avenue de l'Observatoire, F-25044 Besançon Cedex, France

Six forming aid formulations were used to assess the nuclear fuel elaboration by means of the powder injection moulding (PIM) process. These formulations were especially designed for actinide powders (UO_2 and MOX) by taking into account the specificities of these powders, in particular any solutions to prevent radiolysis. Once the feedstocks with the UO_2 powder had been prepared, the thermal studies showed no significant endothermic or exothermic reaction, which demonstrates the quasi independent behaviour of the polymer system with re spect to the uranium dioxide powder. The mass of the carbon residues a key criterion in selecting a formula tion was below 150 ppm for all six formulations, which is still sufficient for obtaining net shaped pellets following the sintering process. The formulations to be recommended for the nuclear fuel application are those containing polystyrene as they achieve satisfactory deagglomeration combined with an adequate level of injectability (low shear viscosity of the system). Moreover, they are theoretically resistant to radiolysis phenom ena due to the benzene rings of the polystyrene.

1. Introduction

Within the frame of the prospective emergence of Generation IV nuclear reactors, processes for fuel manufacturing are reconsidered. In deed, the current fabrication process may hinder innovation in the field of future nuclear fuels if it is not modified or at least completely reviewed [1]. The expected improvements particularly concern 1) sim plifying the current process to reduce the radiological impact on opera tors, 2) consolidating the robustness of the process with respect to shape requirements and to dimensional tolerances, and 3) enhancing the production rate. Using an injection moulding process to manufac ture nuclear fuel is being considered in this specific context.

Outside the nuclear industry, the powder injection moulding (PIM) process is used for the mass production of net shape parts at low cost [2]. This process also has the advantage of being able to produce metal [3] and ceramic parts [4] with complex, variable geometries with an ac curate control of dimensional tolerances [5]. The PIM process involves hot filling a tool (mould) of the desired shape with a mixture of the forming aids and powder [6]. The mixture, referred to as 'feedstock', is cooled and then the forming aids are removed (debinding step) in order to start the densification process through the diffusion in solid state [7,8].

The main objective of using the injection moulding process is to sim plify the current process. Firstly, the fact of introducing forming aids would make it possible, upstream, to restrict the powder preparation operations (crushing, mixing, etc.) and to eliminate the dispersal of con taminating and irradiating powder (reducing the radiological exposure of operators). Moreover, the possibility of directly manufacturing net shaped pellets after the sintering step is a major advantage which would suppress the grinding step involving post sintering abrasion, a very impacting process from a radiological viewpoint in the nuclear field. Lastly, the process offers a wide range of applications, whether in terms of the shape of the fuel or the chemical nature of the powders to be implemented. The PIM process therefore provides advantages as regards flexibility with respect to new designs, and therefore increases the number of innovation possibilities.

However, using actinide powders in the PIM process involves study ing certain scientific subjects which represent a number of potential hurdles to overcome. The latter are directly related to the three main specificities of these powders. Firstly, the morphological characteristics of the actinide powders to be implemented are relatively different from the characteristics of the powders generally used in this process [8,9]. Moreover, the potential chemical interactions between the powder and the forming aids must be identified and their effects must be deter mined. Lastly, the impact of the radiolysis of the forming aids (modifica tion of their properties under the effect of ionising radiation) must be precised. The purpose of the work described in this paper is therefore to determine the feasibility of the powder injection moulding process applied to the manufacture of nuclear fuel through the development of forming aid formulations adapted to the specificities of actinide powders.

* Corresponding author. Tel.: +33 4 42 25 74 63; fax: +33 4 42 25 48 86.
E-mail address: carine.ablitzer@cea.fr (C. Ablitzer).

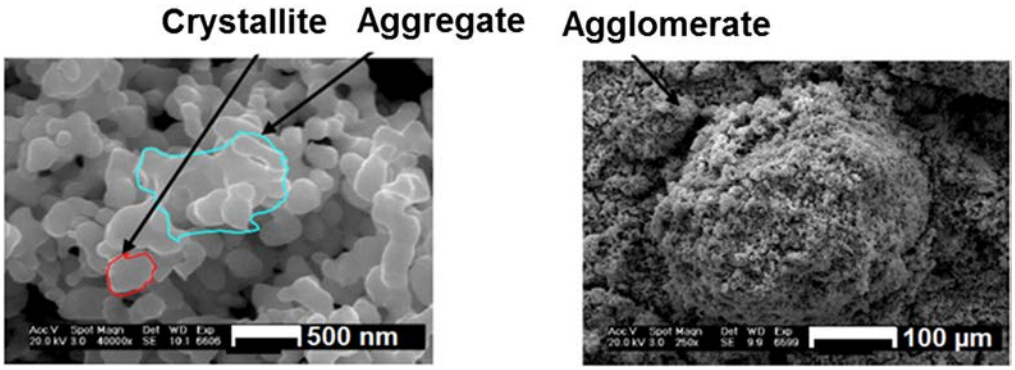

Fig. 1. SEM micrographs of the UO_2 used in the study.

2. Methodology — materials

2.1. Methodology

The issue at hand calls for a methodology based on an accurate scien tific approach making it possible to process the three specificities of the actinide powders mentioned below.

2.1.1. Specificity 1: morphology of actinide powders

At present, the characteristics of actinide powders intended for future fuels have not been defined in a definite manner as fabrication processes may change. However, the characteristics of powders used for preparing the feedstock remain a key decisive element. Therefore, understanding how they affect the process is a major issue for PIM.

To do so, simulating alumina powders broadly covering the morpho logical characteristics of actinide powders have been implemented with a reference forming aid formulation. Results obtained by J. Bricout [10] revealed their suitable behaviour with respect to the injection moulding process on the following levels: preparation of highly loaded mixtures (>50 vol.%), rheological behaviour (shear thinning) and debinding/ sintering capacity.

This study aims to validate these conclusive results with actinide powders. To do so, uranium dioxide powder has been used, since it is the main component of the various oxide fuels currently employed. The possibility of preparing homogeneous highly loaded feedstocks and the rheological behaviour of the forming aid/UO_2 mixtures are analysed herein.

2.1.2. Specificity 2: chemical interactions between UO_2 and the forming aids

The actinide powder was in contact with organic products from the mixing step up to the debinding step. The mixing and injection steps were performed at a temperature of around 180 °C, while the debinding step was performed at around 600 °C. Several types of interactions can occur between the actinide powder and the forming aid throughout the process.

An indirect assessment based on a comparative approach was imple mented to understand these interactions. For this purpose, each compo nent was studied independently and then in the feedstock. We could therefore i) determine the influence of UO_2 on the behaviour of the feedstock at the temperatures implemented during the process (poten tial reactions), ii) characterise the UO_2 powder following the debinding step (observed phases, alterations of the fissile phase), and iii) charac terise the material following the sintering step (density, carbon residues, etc.).

2.1.3. Specificity 3: radiolysis

Radiolysis is defined as the decomposition of organic matter under the effect of ionising radiation from the actinide powders (in our case). According to the chemical nature of the forming aids, such ionis ing radiation has a different impact.

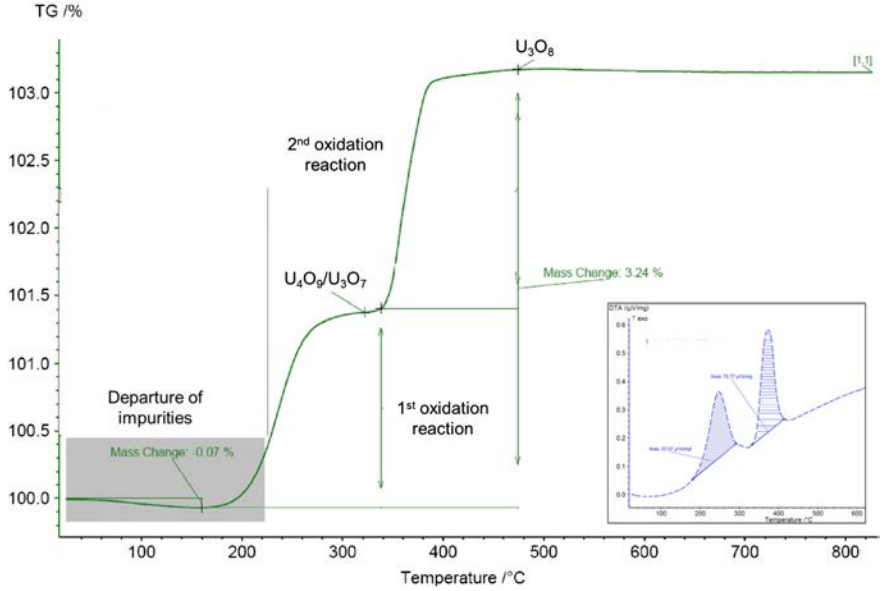

Fig. 2. Thermogramme and differential thermal analysis of UO_2 in a reconstructed air atmosphere (ramp: 10 °C/min up to 900 °C).

Remedial formulations will be implemented by incorporating either a radiolytic decoy and/or radiation resistant molecules. As opposed to the molecules considered as resistant, the radiolytic decoy can be used to absorb the energy from the radiation to preserve the remainder of the system. In this study, these remedial formulations will be prepared and the feasibility of their implementation will be tested. Any formulation that proves compatible with the process will need to demonstrate the effectiveness of these preventive solutions via tests (not covered in this study) with ionising powders representative of the fuel, i.e., plutonium oxide type fuel (MOX).

2.2. Actinide powder used in the study

2.2.1. Selection of the actinide powder: UO_2

Uranium dioxide (UO_2) was selected as the powder for the interaction tests. It is formed by a dry manufacturing process. This powder is depleted in isotope ^{235}U (^{235}U wt.% = 0.3) so that the irradiating phenomena especially those causing the radiolysis of organic matter will not have a significant impact. Only the characteristics of the UO_2 powders, together with the physicochemical effects observed between the powder and the forming aids, will be evidenced.

2.2.2. Morphological and physical characteristics of uranium dioxide

Uranium dioxide powder generally consists of three compounds, as shown in Fig. 1 by the photos taken with a scanning electron microscope (Philips XL30 FEG):

Crystallites: The smallest components which can be identified with a SEM such as shown in Fig. 1 (submicronic size).

Aggregates: Clusters of pre sintered crystallites (strong bonds which are practically unbreakable) with a non convex shape.

Agglomerates: Groups of aggregates formed especially by Van Der Waals forces (weak bonds).

The UO_2 powder used for the study comprised deformed agglomerates of sizes varying from 10 to 200 μm, aggregates around a micrometre and crystallites with an average size of 0.3 μm.

The morphological characteristics of the UO_2 powders were very different from those of powders generally implemented in the PIM process. The differences mainly concern the size and the shape of the particles and the state of powder agglomeration. Considering the importance of the morphological characteristics of the powders in relation to the behaviour of the feedstock, it is legitimate to question their impact on the successful implementation of the process.

2.2.3. Chemical characteristics

During its storage in an air atmosphere, UO_2 oxidises into UO_{2+x}. The initial over stoichiometry must be taken into account. The chemical state of uranium dioxide will, however, change during the process, according to the temperature and atmosphere to which it is exposed. At 600 °C, which represents the highest temperature to which it will be exposed (during the debinding step), it will oxidise into U_3O_8 in an air atmosphere and will be reduced into $UO_{2.00}$ in a reducing atmosphere. These chemical state changes cause variations in powder's mass and volume which must be controlled [11], especially when determining the residual mass at the end of the debinding step and obtaining a complete pellet (at the end of sintering).

Table 1
Characteristics of the forming aids selected to prepare the formulations.

Polymer	Name	Molar mass (g/mol)	Density
Polypropylene	PP1	12,000	0.9
Polypropylene	PP2	190,000	0.9
Low density polyethylene	LDPE		0.93
Polymethyl methacrylate	PMMA	120,000	1.18
Polystyrene	PS2	192,000	1.06
Polystyrene	PS1	35,000	1.06
Paraffin wax	PW		0.9
Stearic acid	SA	284.84	0.94

Table 2
Characteristic temperatures and residual masses determined by TG/DTA for the different forming aids tested to prepare the formulations.

	$T_{melting}$ (°C)		$T_{start\ of\ decomposition}$ (°C)		$T_{end\ of\ decomposition}$ (°C)		Residual mass (%)
	N_2	ArH_2	N_2	ArH_2	N_2	ArH_2	ArH_2
PP1	155	156	280	295	475	477	0
PP2	164	165	353	360	483	480	0
PEBD		112		380		495	0.1
PS1	Tg = 125		283	307	460	465	0
PS2	Tg = 125			337		455	0
PW	72	74	225	236	470	470	0.1
PMMA	Tg = 105			233		443	0.7
SA	73	74	220	220	355	410	0

Tg = temperature of vitreous transition.

2.2.4. Determination of over stoichiometry

The degree to which uranium dioxide powder oxidises does vary during its storage in an air atmosphere. It is therefore very important to determine the over stoichiometry of the powder when it is implemented in the process. At ambient temperature in an air atmosphere, the O/U ratio of the UO_2 powder increases according to the storage time [12,13].

In order to determine the O/U of the dry UO_2 powder employed, we conducted a thermogravimetric analysis (TGA) together with a differential thermal analysis (DTA) on about 200 mg of gross powder in an oxidising atmosphere (reconstructed air). The thermal cycle consisted of a temperature increase of 10 °C/min up to 900 °C where a 1 hour plateau was observed. The cooling rate imposed was 10 °C/min. The aim was to transform UO_{2+x} into stable U_3O_8 according to the following reaction: $UO_{2+x} + y\ O_2 \rightarrow UO_{8/3}$. Fig. 2 illustrates the analysis results.

The difference in mass explained by the oxidation makes it possible to calculate the initial stoichiometry. We were also able to confirm that U_3O_8 was stable in air because no reaction was observed from 500 °C and during the cooling phase. The total mass gain, once the impurities had been eliminated, amounted to 3.25%. This mass increase, lower than the theoretical mass increase (3.95%), highlights the over stoichiometry of the powders employed, which amounts to $X = 0.115 \pm 0.007$. The uranium oxide employed was therefore similar to $UO_{2.11}$.

2.3. Forming aids

2.3.1. Selection criteria for the forming aids

Selecting the forming aid formulation is essential to ensure the successful completion of the PIM process. Although they do not contribute to the final composition of the pellets, the forming aids play a major role in the success of the overall process [14]. The aim of the formulation is to transport the powder into the mould so it can be shaped. The formulation consists of a polymer with a structure ensuring the mechanical resistance of the pellet up to the densification step (binder agent), a low

Table 3
Six forming aid systems assessed in the study.

	Binder	Plasticizer	Radiolysis addition	Surfactant	Proportion vol.%
Fa	LDPE	PW		SA	40:55:5
Fb	PP1	PW		SA	40:5:5
Fc	LDPE	PP2		SA	40:55:5
Fd	PS2	PW		SA	40:55:5
Fe	LDPE	PW	PS	SA	31.6:43.4:20:5
Ff	LDPE	PW	PMMA	SA	31.6:43.4:20:5

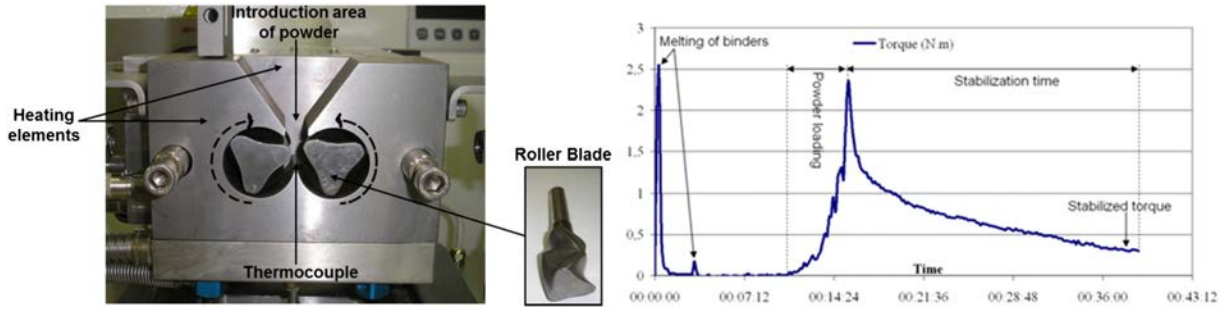

Fig. 3. Two-blade mixer in open position — standard behaviour of the mixing torque when operating.

viscosity component facilitating the injection step (plasticizer), and dis persing, lubricating or surfactant type additives in small quantities.

The stresses induced by the actinide powders rule out the use of some types of forming aids. We have used thermoplastic systems con taining polyolefins and wax as the forming aids for the implementation of the UO_2 powders.

Little information is available on the radiolysis of polyolefins, but it is clear that certain polymers are more resistant than others, and that cor rective measures are also possible [15]. By taking into account the above mentioned information and a state of the art review [16] it was possible to select the polymers for the formulation of the forming aid apparently suitable for actinide powders. This information is listed in Table 1.

PP and the PEBD are very commonly used polymers in injection pro cesses, whether for injecting thermoplastic products alone or for injecting powders [17]. Their behaviour has already been largely tested and a great amount of feedback is available. According to available data, LDPE also behaves much better with respect to radiolysis phenomena than PP. Like SA, PW is one of the most widespread and effective plasti cizers when used as a surfactant. PS was selected because it potentially represents the thermoplastic polymer with one of the best behaviours with respect to radiolysis due to the presence of benzene rings. PMMA was selected for the opposite reason, namely its low resistance to radi olysis due to which it could be used as a radiolytic decoy to preserve the other forming aids. As the types of the forming aids have been defined, their function in the formulation will especially depend on the molar mass and thus on the viscosity of the polymer in question.

2.3.2. Thermal characterisation of the forming aids

All of the selected polymers underwent thermogravimetric analysis and differential thermal analysis (ATG/ATD), which made it possible to analyse the behaviour of the polymers during a thermal cycle in a given atmosphere. The purpose of these analyses was to determine the char acteristic temperatures of each polymer (melting temperatures and start and end of decomposition temperatures) on the one hand, and their behaviour during thermal degradation (including analysis of the gases emitted) on the other hand. Knowing these parameters is very important because they are used to determine:

- possible polymer combinations for the implementation of formulations,
- the residual masses at the end of the debinding cycle,
- the mixing temperature (temperature higher than the highest melting temperature and lower than the lowest degradation temperature),
- the optimised sintering cycle (to gradually eliminate the com ponents and determine the temperature plateaus in order to preserve pellet integrity).

In this study, the atmospheres employed were nitrogen (N_2), which was the mixing atmosphere (generally used for inerting the glove boxes) and a mixture of argon hydrogenated at 5 vol.% of hydrogen (Ar 5%H_2), which was the debinding atmosphere to prevent the oxida tion of UO_2 into U_3O_8. The characteristic temperatures ($T_{melting}$, $T_{start\text{-}of\text{-}decomposition}$ and $T_{end\text{-}of\text{-}decomposition}$) as well as the residual mass are indi cated in Table 2.

The start of decomposition temperatures under N_2 were compatible with the mixing temperatures (175 °C for a formulation containing PP or PS and 145 °C for a formulation containing PE). In hydrogenated argon, the thermal decomposition of all polymers, except for PMMA, can be regarded as complete. There was no significant measurable resid ual mass under the conditions tested. These results therefore show that all the selected polymers are likely (at least with respect to this criteri on) to be incorporated into a forming aid formulation because, theoret ically, they will leave very little residue after the thermal debinding step.

2.4. Selection of the forming aid formulations

Six forming aid formulations were chosen according to the charac terisation of the polymers. Based on the thermal and rheological data, PP2, PS2 and LDPE were chosen as the binding agents (or binders) to

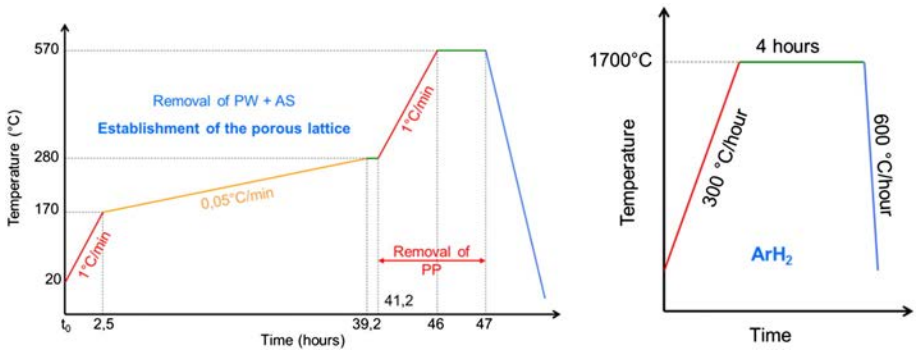

Fig. 4. Thermal cycle for debinding (left) and for sintering (right).

Table 4
Maximum melting temperatures, minimum decomposition temperatures of components and mixing temperatures for the six formulations used to make the dry UO_2 feedstocks.

T (°C)	Fa	Fb	Fc	Fd	Fe	Ff
$T_{melting}$	112	165	155	125	125	112
$T_{decomposition}$	220					
T_{mixing}	145	175	175	175	145	145

Table 5
Increments of torque with the load factor for the six formulations used to make the dry UO_2 feedstocks.

ΔM (%)	Fa	Fb	Fc	Fd	Fe	Ff
40 vol.%–45 vol.%	51.9	44.4	36.7	38.5	59.4	54.8
45 vol.%–50 vol.%	35.7	38.6	35.5	53.6	46.7	46.2

ensure the bonding properties of the system (which will be eliminated last).

PP1 and PW were chosen as the plasticizers to make the polymer system more viscoelastic by modifying its plasticity. These plasticizers can be described as smaller chains which insert themselves between the binder chains. Their molecular mass is lower than the binders.

Stearic acid was chosen as the surfactant (or dispersing agent), which theoretically provides better contact and binding between the powder and the forming aid system thanks to its two functional groups: a polar group interacting with the powder and a non polar group with strong affinities with the polymer system.

The PS1 and PMMA compounds were selected for their capacity to prevent radiolysis phenomena.

The difference between the start of decomposition temperatures of the plasticizer and of the binder must be sufficiently high (at least 100 °C) to allow the separate removal of the two polymers. Therefore, two polymers of the same nature cannot be used as a plasticizer and as a binder because their start of decomposition temperatures would be too similar. Therefore, PP1 and PP2 cannot be combined as their start of decomposition temperature would only differ by 65 °C in Ar 5%H_2. The six forming aid systems chosen and adapted for the UO_2 powder are listed in Table 3.

3. Experimental procedure

3.1. Polymer/powder mixing

The feedstocks were mixed in a BRABENDER®Plasti Corder® two screw mixer (50 series) as shown in Fig. 3. For the requirements of the study, the mixer was adapted for a nuclear environment in an inert glove box so it could be used to make actinide based powder mixtures. The rotating speed of the blades was set at 30 rpm and the working atmosphere was nitrogen (N_2). The forming aids were first added to the pre heated tank before the powder was added according to a specific protocol. This mixer could also be used to develop and analyse feedstocks. It was possible to monitor the mixing torque and the temperature variations during the mixing process, which provided information on the key parameters of the feedstock such as the steady state torque (Fig. 3) and the critical load factor.

3.2. Analysis of feedstocks

3.2.1. Rheological analysis

The rheological characterisation of a feedstock is required to determine its injectability on the basis of its viscosity and homogeneity among others. We used a Malvern RH2000 twin bore capillary rheometer to characterise the feedstock. The rheological analyses were performed at 220 °C using a die with a diameter of 2 mm and a length of 32 mm equipped with a 70 MPa extrusion pressure transducer. This equipment thus made it possible to study the viscosity with a shear rate ranging from 1 to 10,000 s^{-1}.

3.2.2. Thermal analysis

The thermal properties and/or any polymer polymer or polymer powder interactions will be determined by means of a NETZSCH STA 409 thermobalance coupled with a quadrupole mass spectrometry making it possible to perform DTG/DTA.

3.3. Fabrication of fuel pellets

3.3.1. Forming by pressing

As the UO_2 laboratory is not equipped with an injection moulding press, a hot press was specifically designed to shape the pellet. This press was used to make pellets with a diameter of 10 mm and a length between 5 and 20 mm. The pressure and temperature applied to the feedstock during the pressing operation were representative of a high pressure injection moulding process: 76 MPa and 220 °C. Working with alumina powders, Bricout [16] has verified a homogeneous shrinkage during sintering of hot pressed pellets, which shows that a good homogeneity of density of powder is obtained with the hot pressing tool.

Though the hot press is suitable pressing, pellet ejection from the die is a very complex operation. The disadvantage of this equipment lies in the difficulty of retaining the integrity of the pellet shape and surface condition during stripping by ejection (a problem that does not exist for standard injection moulding presses).

So, the hot press is considered to give pellets rather representative of PIM but it can lead to shape or surface defects, leading to final dimensions after sintering potentially less good.

3.3.2. Debinding and sintering

Pellet debinding was performed exclusively by thermal means. A tube resistance furnace was therefore used for the debinding of 20

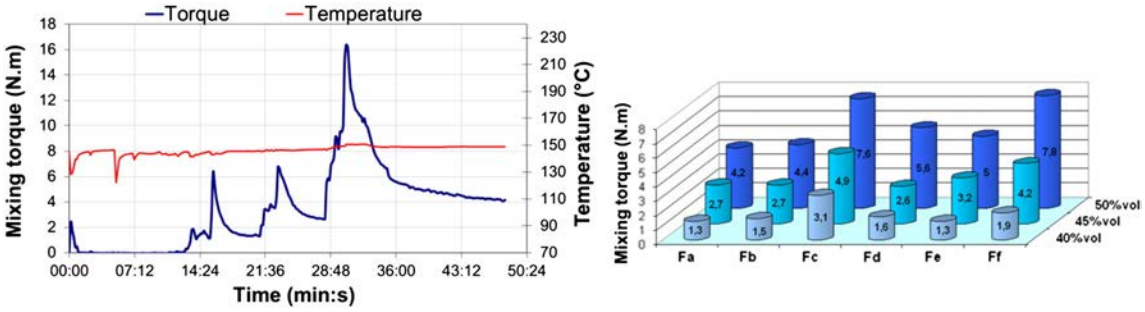

Fig. 5. Mixing behaviour of Fa feedstock loaded with 50 vol.% of dry UO_2 (T = 145 °C, V_{blades} = 30 rpm, steady-state torque at 0.5 N·m); steady-state mixing torques for the 6 feedstocks loaded with 40, 45 and 50 vol.%.

Table 6
Estimation of the stresses applied to the powders of the six feedstocks during mixing.

Feedstock	Fa	Fb	Fc	Fd	Fe	Ff
Relative stress (kPa)	109	90	475	53	95	313

pellets per batch. All debinding cycles for this study were performed under an argon atmosphere with 5% hydrogen (Ar 5%H_2) to overcome the oxidation phenomena of the UO_2 powder.

Pellet densification was performed in a high temperature furnace in Ar 5%H_2.

The debinding and densification cycles by diffusion in solid state (sintering) for the fuel pellets are shown in Fig. 4.

3.4. Pellet analysis

3.4.1. Pellet metrology

To determine the pellet diameter, a profile of the entire pellet length was taken with a pitch of 1 mm by starting from the top of the pellet to assess the diameter variations as best possible. A ZYGO 1202B laser micrometre was used. The calculation of uncertainties produced a result of 0.0035 mm.

The height was measured using a HEIDENHAIN MT12B sensor which produced a result with an accuracy of ±0.015 mm.

3.4.2. Pellet density

The hydrostatic density by alcohol absorption was used to calculate the pellet density without any assumption of shape and to deter mine the type of porosity (open or closed) and the void ratio.

3.4.3. Microstructural analysis

The pellets were cut up, coated and polished so their microstructure could be analysed by a number of different microscopic methods (opti cal and SEM). Etching was performed to reveal the microstructure, which was then followed by SEM observation (Philips XL30 FEG) with chemical contrast (back scattered electrons).

X ray diffraction (XRD) with a Bruker D8 Advance was used to identify the different phases.

3.4.4. Residue analysis

The residues could be analysed by thermogravimetric means accord ing to the mass variations during the total oxidation of the UO_2 powder and the related carbon.

The second method used was able to accurately assay the carbon by means of a LECO infrared carbon analyser. This method was used to determine the quantity of carbon in the solid samples. The assaying range for carbon was [2 ppm 40,000 ppm] with an accuracy of ±20 ppm.

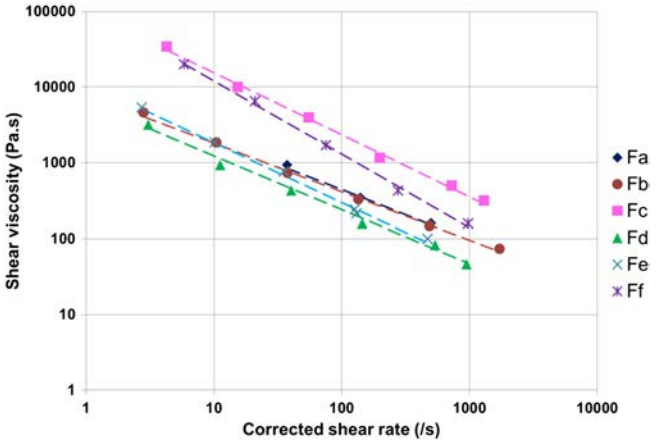

Fig. 7. Rheological behaviour of the six feedstocks (points correspond to experimental values and broken lines to the power law model).

4. Results and discussion

4.1. Implementation of feedstocks (behaviour during mixing)

The UO_2 powder and forming aids were mixed in identical propor tions of volume. The volume load factor was therefore 50%.

The mixing temperatures of six formulations were determined by characterising the polymers alone in nitrogen (Table 2). The mixing temperatures of different feedstocks were determined by compromis ing between the highest melting temperature and the lowest decompo sition temperature of the polymers comprising the formulation. This data is given in Table 4. In the remainder of the document, the term 'Fa feedstock' refers to a mixture using the formulation 'Fa' loaded with 50 vol.% of dry UO_2 powder; ditto from Fb, Fc, Fd, Fe and Ff.

4.1.1. Behaviour during mixing

Torque rheology can give useful information on the evolution of the mixing process between the powders and the binder system. Torque values are also related to viscosity and can give and idea of how well a feedstock flows. In high particle solid loading binders, friction between particles plays an important role in the viscosity and mixing behaviour. The packing capacity of a powder will also determine the maximum solid loading. Unlike spherical powder, irregular particle contacts occur along surfaces instead of points, increasing the viscosity. These types of powders also show a low packing capacity which causes high viscosity. In the case of UO_2 powder there is also the problematic of high agglomeration. Agglomerates may reduce drastically the packing capacity and thus produce an increment of the viscosity. Moreover, if these agglomerates are not broken during mixing they might cause de fects in the subsequent stages of PIM. Agglomerate breakage can occur by hydrodynamic forces exerted by the binder or by erosive effect of contacts between agglomerate clusters or particles. A low viscosity

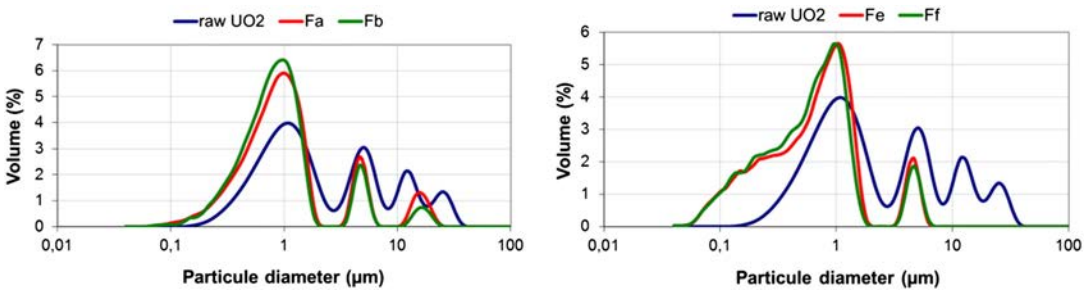

Fig. 6. Grain-size distribution of the gross dry UO_2 powder and dry UO_2 powders resulting from the Fa and Fb feedstocks after the mixing and debinding phases.

Table 7
Parameters of the power law ($\eta \quad m\dot{\gamma}^{n\ 1}$) for the six feedstocks.

Feedstock	Fa	Fb	Fc	Fd	Fe	Ff
m (Pa·s)	9227	7917	102,243	6335	11,335	113,224
n	0.34	0.36	0.18	0.29	0.21	0.03

binder will cause less effect on the agglomerate breakage than a high viscosity one. As the solid loading is increased, less mobile binder is present but the erosive effect will increase. These kinds of effects may be identified by studying torque curves during mixing. In this study, the same quantity of powder was added from time to time according to the same protocol for all six tests. Furthermore, the steady state mixing torques at 40 vol.%, 45 vol.% and 50 vol.% of powder were determined so they could be compared according to the formulation in question. The mixing behaviour of the Fa feedstock was extremely representative of the 5 other feedstocks and is shown in Fig. 5. The diagram summarizes the steady state torques for the six different feedstocks.

The steady state torques and the feedstock adding times were different. These differences were due to the type and viscosity of the polymers used. The critical and optimal load factors were therefore different for each feedstock.

The Fa and Fb feedstocks had practically the same mixing torques. The differences between the two lie in the type of binder and the mixing temperature. Low density polyethylene (LDPE) at 145 °C has a shear viscosity similar to that of polypropylene 2 (PP2) at 175 °C, which was confirmed by the rheological analysis of polymers (not discussed in this study, see [16]). It is not possible to increase the mixing temperature above 175 °C without deteriorating the stearic acid (start of decomposition under nitrogen at 220 °C). However, it is possible to increase the mixing temperature of the Fa feedstock to 175 °C without any deterioration. This temperature increase seems to thin the system even more, thereby increasing the critical load factor. The Fa formulation thus has an advantage from a rheological viewpoint compared with the Fb formulation. However, a decrease of the binder viscosity may cause a less effective agglomeration breakage effect as it will be discussed in subsequent paragraphs.

Comparison of the Fa, Fe and Ff feedstocks mixed at the same temperature of 145 °C shows that adding polystyrene or polymethyl methacrylate (PMMA) even at low molecular weights does not have the same impact on the mixing torque. A heightened increase in the torque can be observed for the Ff feedstock (containing PMMA), while the steady state torques of the Fe feedstock (containing polystyrene) are slightly higher than those of the Fa feedstock. As previously explained, the flow of these three feedstocks can be increased by raising the temperature to 175 °C.

The Fa and Fc feedstocks differed by their type of plasticizer and by the mixing temperature. The use of polypropylene (PP1) as plasticizer multiplies the mixing torque by two compared with paraffin despite a higher mixing temperature. Paraffin therefore thins the system while polypropylene improves bonding (the shape is better preserved). A compromise between the two effects must be found so as to optimise the formulations.

The mixing torque of the Fd feedstock shows that it is possible to use polystyrene as a binder. Its combination with paraffin and stearic acid was unusual since it is hardly mentioned in literature.

Lastly, the six formulations could be mixed with a steady state torque at the end of mixing for a load factor of 50 vol.%, which leads us to believe that the powder was homogeneously dispersed in the polymer system. This fact does not necessarily mean that the agglomerates were broken. In Table 5, the increment of torque from 40 vol.% to 45 vol.% is compared with the increment of torque from 45 vol.% to 50 vol.%. As the solid loading increases close to the maximum value that a binder can accept, the increment of torque per volume of powders added is expected to increase. However, for all feedstocks except Fc and Fd, the increment of torque from 45 vol.% to 50 vol.% is less than the increment of the previous adding step. This fact suggests that a breakage of agglomerates occurs more effectively in the mentioned compositions as consequence of an increment in the erosive effect due to a reduction of mobile binder in the system. As the agglomerates break, the packing capacity of the powders increases and the viscosity is reduced. The effectiveness of agglomerate breakage is discussed in the following section.

4.1.2. Deagglomeration analysis

The mixing stage provoked a change in the initial powder characteristics owing to the stresses generated by the rotating blades of the mixer. The model developed by Canedo [18] based on the circumferential flow around the blades of the mixer makes it possible to deduce the stress generated inside the system, as listed in Table 6.

The differences in the mixing torques which depend on the formulation suggest that deagglomeration of the dry UO_2 powder will occur in a significantly different manner depending on the forming aid formulations.

With the objective of detecting the influence of the reference formulation on the impact of mixing on the initial UO_2 powder characteristics, particle size analyses before and after mixing were performed on the feedstocks in question. To do this, the granules of each feedstock were given a short thermal debinding cycle so as to study the grain size distribution of the resulting powder by laser granulometry in wet conditions (Beckman Coulter LS 13320 device).

This study covers two extreme cases of deagglomeration represented by the Fa and Fb feedstocks on the one hand, and the Fe and Ff feedstocks on the other hand. The behaviour of the Fc and Fd feedstocks is somewhere between these two extremes. Comparisons of grain size distributions are shown in Fig. 6.

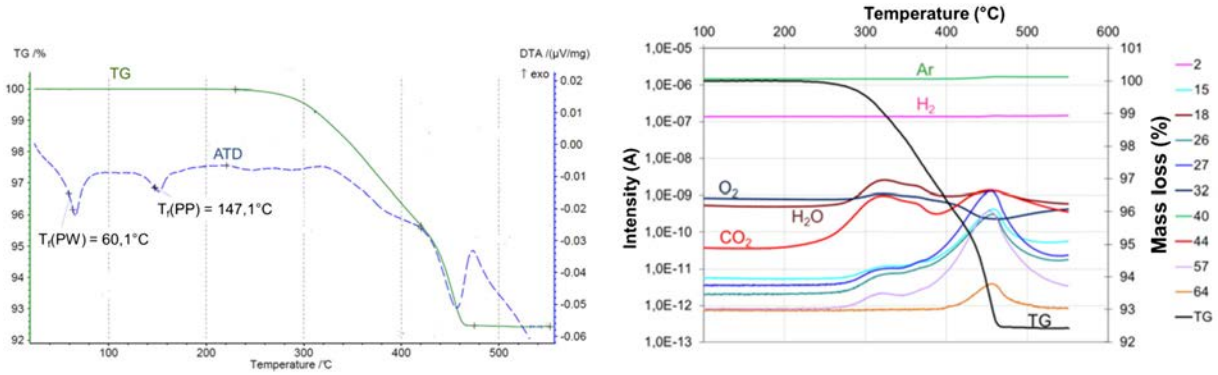

Fig. 8. DTG/DTA signals for the Fb formulation during the debinding cycle; DTG signal coupled with gas analysis of the Fb feedstock during the debinding cycle.

Table 8
Comparison of melting temperatures (°C) of polymers alone or mixed in a feedstock.

	LDPE	PP2	PW	PP1
Polymer only	112.4	165.4	74.5	155.8
Fa	97.8		58.9	
Fb		147.1	60.1	
Fc	108			155.6
Fd			59.8	
Fe	97.6		57.7	
Ff	95.9		58.8	

4.1.2.1. Fa and Fb formulations. As can be observed in Fig. 6, deagglomeration results in three grain size classes only, which are very distinct this time:

a class centred on 1 μm like the gross powder but whose proportion has clearly been increased (from 4% to about 6%),
a class centred on 4.6 μm like the gross powder,
The last grain size class is centred on 15 μm and is found in a very small proportion.

The stress generated during mixing provoked the deagglomeration of the largest agglomerates and therefore the increase in the proportion of millimetric sized aggregates. The mean diameter also decreased; from 1.64 μm for gross powder to 0.97 μm and 0.89 μm for the Fa and Fb formulations respectively.

4.1.2.2. Fe and Ff formulations. The grain size distributions after the mixing and debinding stages (short thermal cycle) are represented in Fig. 6. A considerable increase in the proportion of crystallites can be observed. In addition, the resulting powders for these two formulations only contain two grain size classes since those greater than 10 μm seem to have disappeared. The mean diameter, D50, therefore greatly decreases and is equal to 0.73 μm for the powder resulting from the Fe formulation and to 0.66 μm for that resulting from the Ff formulation.

The choice of formulation therefore has a significant impact on the mixing behaviour of dry UO_2 powder. The effect of deagglomeration differs according to the formulation in question.

Firstly, these differences can be mainly explained by the stress during the mixing of the powder and of the forming aid formulation.

Nonetheless, the intensity of stress during mixing cannot alone explain the appearance of crystallites in the Fc, Fe and Ff feedstocks. As the crystallites are pre sintered, the stress on the particles generated by mixing seems to be relatively moderate making it difficult to clearly conclude on the established possibility of failure of necks formed during sintering. To refine the interpretations resulting from the particle size analysis, additional specific surface and microscopic analyses would be needed to reach a more definitive conclusion.

These results nonetheless highlight the differences in the bonding of aggregates or agglomerates comprising the dry UO_2 powder. The first two populations of the dry UO_2 powder centred on 1 and 7 μm 'resist' the stress induced by the mixing operation in all cases. Therefore, the aggregates of a size around one micron do result from the pre sintering of crystallites between themselves, which renders them indivisible. The aggregates represented by the population centred on 7 μm are also indivisible. This phenomenon can either result from the pre sintering of crystallites (like in the previous case), or from the agglomeration of 1 μm aggregates with sufficient bonding which prevents them from being disintegrated by the stress induced by mixing. The agglomerates of the two other populations are divisible and formed of aggregates with sizes nearing a micrometre. Their disappearance does indeed coincide with the increase in the population centred on 1 μm, whereas the population centred on 7 μm remains unchanged. It is therefore possible to propose a deagglomeration mechanism for the dry UO_2 powder on the basis of these interpretations: deagglomeration occurs when agglomerates disintegrate into aggregates (increase in the population of 1 μm aggregates) with the combined effect of the erosion phenomenon causing an increase in the number of very fine particles.

4.2. Analysis of feedstock injectability

The injectability of the six feedstocks in question was investigated by capillary rheology. The injectability criteria taken into account were 1) the flowability through a 2 mm die, 2) the development of a shear thinning behaviour, and 3) a viscosity of around 1000 Pa·s for a shear rate of 100 s^{-1}. The temperature of the rheological measurements (220 °C), corresponding to the temperature used for the pressing step, is the start of noticeable decomposition of SA, so heating durations have been minimized.

The results are shown in Fig. 7. The results have been modelled by a power type law over the [1 1000 s^{-1}] shear rate range. The parameters of the analytical models are listed in Table 7.

The six formulations meet the injectability criteria. The most viscous feedstock (Fc) is that which uses low molecular weight polypropylene as the plasticizer instead of wax. Combined with the Ff feedstock, however, the Fc feedstock will be rather difficult to inject, considering their high shear viscosity. In this case, the flow is also through a die with a 2 mm diameter and it will be more complicated to ensure the flowability in a 1 mm or even a 0.5 mm diameter die with these two feedstocks.

The least viscous feedstock (Fd) at the relevant temperature of 220 °C is that using polystyrene as the binder. The feedstocks composed of the Fa and Fb formulations show a very similar rheological behaviour. Adding 20% of polystyrene to the Fa formulation does not change the low shear rate behaviour. The beginnings of a Newtonian plateau region nonetheless appear from 1000 Pa·s.

According to past research, the fact that all the feedstocks flow when they are 50 vol.% loaded means that the critical load factor of these feedstocks is at least equal to 54 vol.%. The critical load factors determined for the Fb and Fd formulations are 58 and 54 vol.% respectively. These values are therefore in agreement with the sintering of dry UO_2. The

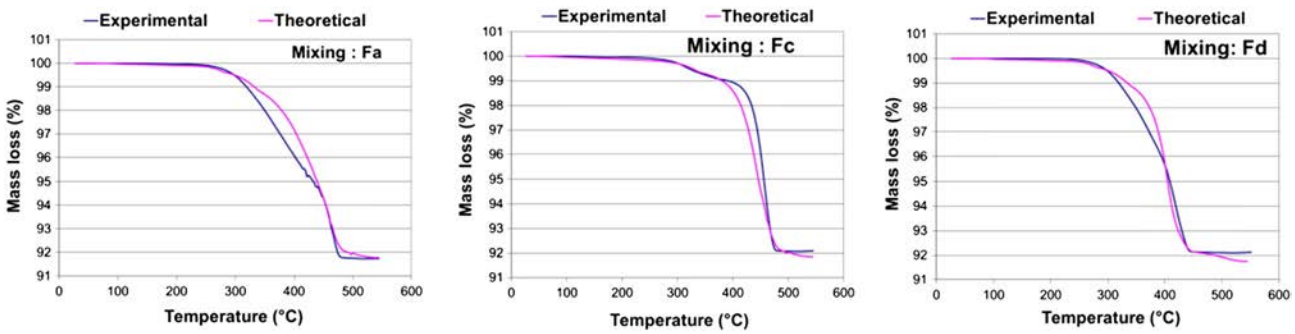

Fig. 9. Comparison of theoretical and experimental curves for the Fa, Fd and Fc feedstocks during decomposition under an accelerated debinding thermal cycle.

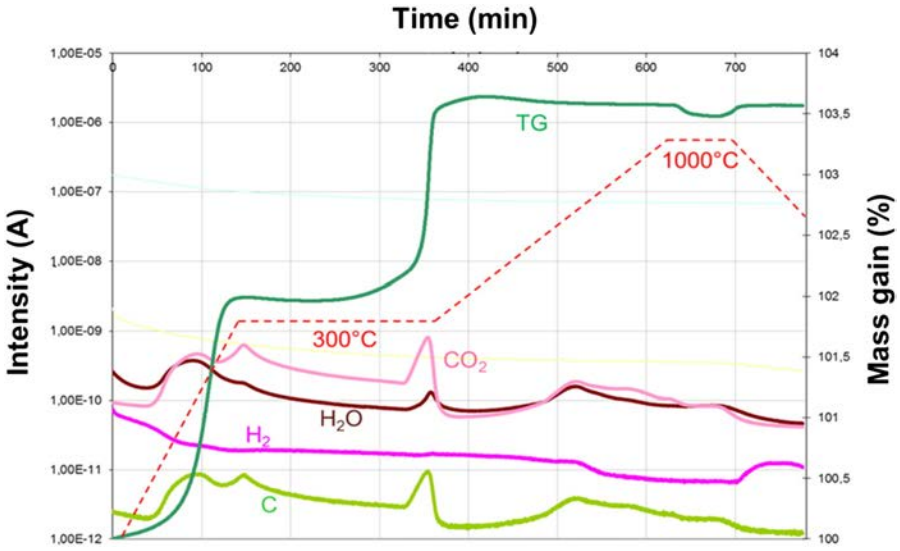

Fig. 10. Oxidising cycle on the powder from the Fa feedstock having undergone debinding.

density of the gross powder compacts after pressing (by standard pow der metallurgical techniques) is between 50 and 55% of the theoretical density.

4.3. Analysis of interactions between UO_2 and the forming aids

An analysis methodology together with an experimental pro gramme was implemented in order to compare the formulations in question. The main objective is to highlight the potential chemical interactions during the different stages of the injection moulding process. There is little available knowledge on interactions between organic compounds and uranium dioxide powders at relatively high temperature.

4.3.1. Thermal characteristics

Differential thermogravimetric and thermal analyses (DTG/DTA) were performed for the six feedstocks loaded at 50 vol.% in a thermal cycle representing an accelerated debinding cycle in ArH_2 (heated at 10 K/min then plateaued for 10 min before dropping back to ambient temperature). The results for the Fb feedstock are shown in Fig. 8, while the five other feedstocks illustrated the same general behaviour.

4.3.1.1. Melting temperatures. Table 8 compares the melting tempera tures of polymers when incorporated in a feedstock with the melting temperatures of polymers alone. This makes it possible to assess the separate behaviour and immiscible nature of polymers mixed in contact with UO_2.

Two distinct categories have been evidenced. The first concerns the Fc formulation the only formulation free of paraffin. The melting tem peratures obtained by thermal analysis of the feedstock are similar. It is therefore possible to affirm that these two polymers (PP and LDPE) are completely immiscible in any proportion and that contact with uranium dioxide has no effect on the physicochemical behaviour at high temper ature in a reducing atmosphere. The behaviour of each polymer even mixed is therefore independent.

The formulations containing paraffin (Fa, Fb, Fd, Fe and Ff) show an offset in the melting peaks tending towards a lower temperature by about 15 °C compared with the components in the formulation.

We must nevertheless take into account a significant difference in the implementation history of the polymers analysed in the feedstocks and those analysed separately. The polymers contained in the feedstock have been subjected to mixing, i.e., mechanical and thermal stress that the polymers alone have not experienced. Such stress levels may have deteriorated the polymers to result in a change in their melting temper ature. It may even be the case that such thermal stress has played a de cisive role in modifying the physical properties of the polymers. We can nevertheless qualify this supposition based on the example of the Fc for mulation which also experienced such stress without any notable im pact on the melting temperature. Yet it is also true that paraffin has a very low melting point compared with PP1, which means its properties are more likely to be modified by the different types of stress encoun tered during the mixing stage.

The immiscibility of polymers in feedstocks in contact with UO_2 therefore seems to have been proved.

4.3.1.2. Degradation behaviour. To determine whether the behaviour of the feedstock is a linear combination in parallel of each of its compo nents, the DTG curves were reconstructed on the basis of curves obtain ed separately for each component of the feedstock (forming aid and powder). These curves are referred to as “theoretical curves” below. These theoretical curves are compared with experimental curves; they show the quasi linear behaviour of each component of the feedstock during degradation for all six formulations. However, some differences observed are explained below and illustrated in Fig. 9.

For the five feedstocks containing paraffin, the experimental curves show that the paraffin degradation rate is higher than in the theoretical curves. The two curves meet during the removal of the primary binder. The behaviour of the paraffin therefore seems to be impacted and un dergoes changes. For the Fc formulation with no paraffin, the two curves practically fit from the beginning of the degradation process. Like for the melting temperatures, these differences in degradation rates can be due to contact with uranium dioxide or due to the implementation history.

4.3.1.3. Interactions between UO_2 and the forming aids. The DTA curves of the Fa, Fb, Fc, Fd, Fe and Ff feedstocks show the same behaviour during the debinding cycle:signal stability up to 300 °C (with endothermic melting peaks) and then a drop in the signal intensity and the appear ance of an endothermic peak. The endothermic peak corresponds the polymer degradation rate at maximum (around 430 °C).

Table 9
Estimation by DTG analysis of the proportion of carbon residue after having removed the binder from the six feedstocks.

	Fa	Fb	Fc	Fd	Fe	Ff
wt.% residue	0.42	0.31	0.38	0.31	0.34	0.44

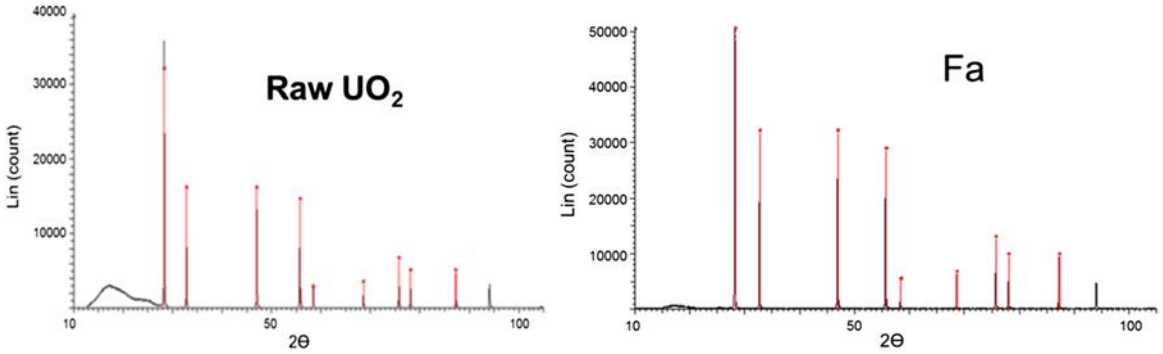

Fig. 11. XRD analysis of the dry UO_2 powder having undergone a short debinding cycle; XRD analyses of the dry UO_2 powder resulting from the Fa feedstock after debinding.

The drop in the signal intensity is due to the change in the thermal conductivity of the sample according to the degree of progress in the polymer degradation. At the start of the test, the system comprises the [sample crucible with load] and [forming aid + empty reference crucible], whereas after the disappearance of the polymer, the system becomes [sample crucible with load] and [empty reference crucible].

According to the resulting thermal analysis curves, there is no reac tion that could prove damaging to the process between UO_2 and the forming aids. Furthermore, the behaviour of the feedstock during degra dation is a linear combination of the behaviours of the components comprising the feedstock.

4.3.2. Analysis of the fissile phase changes

The changes in the fissile phase (uranium oxide) can be determined by analysing the residues after debinding, as well as the crystallography phase changes.

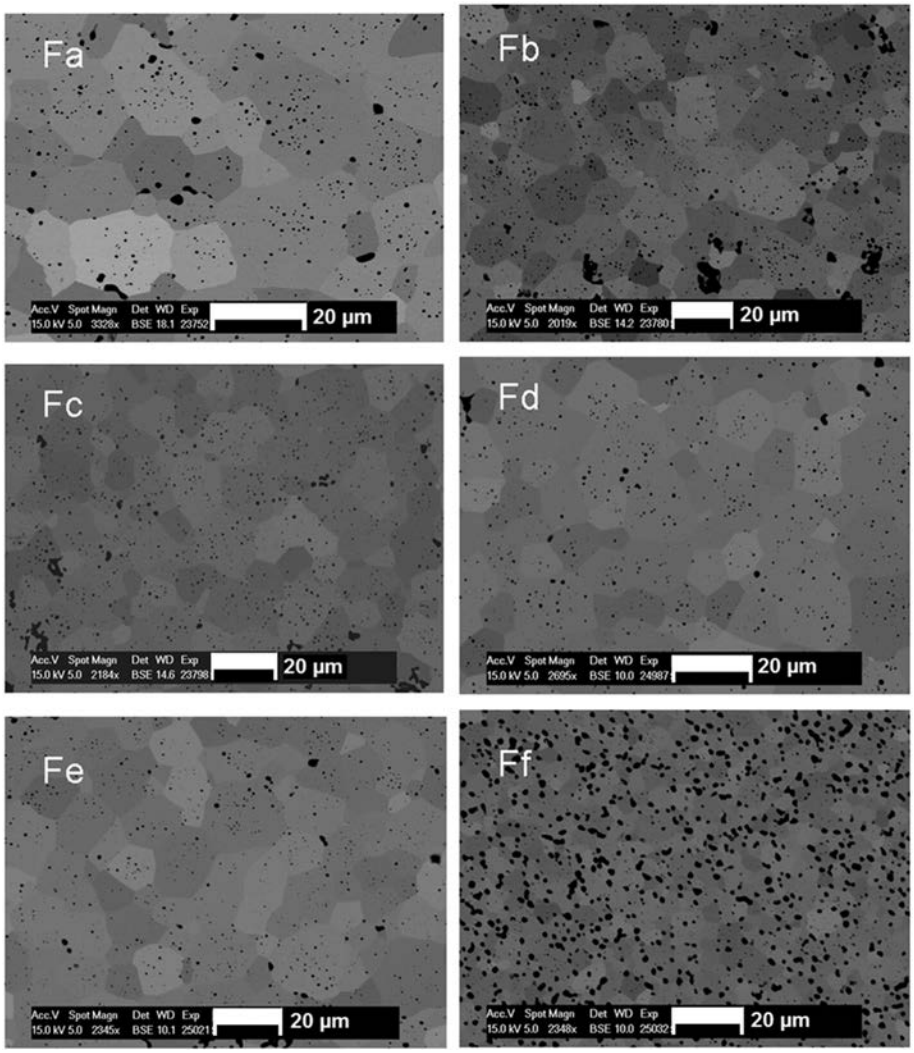

Fig. 12. Comparison of the final microstructures of densified pellets (fabricated under the same conditions) resulting from the six feedstocks.

Table 10
Determining the residual quantity of carbon in the pellets resulting from the six feedstocks.

	Fa	Fb	Fc	Fd	Fe	Ff
C content (ppm)	155	141	114	113	112	129

4.3.2.1. Analysis of residues after debinding. A thermal oxidation cycle was applied to the powders resulting from the debinding of the six feed stocks. The thermal cycle included a plateau at 300 °C and then a tem perature rise to a maximum of 1000 °C. The general behaviour was the same for all powders. We have illustrated the example of the pow der resulting from the Fa formulation. The results on the mass gain and the related gas analysis are shown in Fig. 10.

The gas analyses clearly show the release of carbon compounds. The mass gain is 3.53% in relation to the initial mass. Comparison of this re sult with the theoretical result (3.95%) of the oxidation of $UO_{2.00}$ into U_3O_8 as discussed in Section 2.2.4 makes it possible to determine the quantity of carbon residue after the debinding phase. Table 9 shows the proportions of residue assessed by this method for the powders from which the binder has been removed.

These results were also confirmed by residue analysis using a carbon analyser. These mass percentages of residue remain high compared with the fuel specification on the carbon content which is 100 ppm. This specification is, however, applicable to sintered pellets, which means that the impact of the sintering stage on the residual carbon con tent remains to be checked.

4.3.2.2. Determination of observed phases. In order to consolidate this conclusion and the fact that the fissile phase has not been modified by the presence of forming aid residues, it must be checked that the behav iour of the UO_2 powder has not been changed under a reducing atmo sphere at high temperature. To do this, XRD analyses were performed on the six resulting powders after the debinding cycle in order to deter mine the observed crystalline phases. Fig. 11 shows the results of the XRD analysis for the UO_2 powder having undergone a short debinding cycle in a reducing atmosphere. The only observed phase was the cubic phase of $UO_{2.00}$. The characteristic peaks of this phase are indicat ed by red pointers.

The XRD analyses of the UO_2 powders after their feedstocks had been subjected to a short debinding cycle show a single observed phase for all six cases, which is that of $UO_{2.00}$ like for the gross UO_2 pow der. The characteristic peaks of several other phases (UC, UC_2, U_4O_9, UO_3, U_3O_8, etc.) which could have been observed were compared with the XRD analyses of the resulting powders. These peaks have not been plotted on the spectra to make the figures easier to read, but no phase other than the $UO_{2.00}$ phase was evidenced within the detection limits of the device. Considering that the six spectra are identical, that of the powder resulting from the Fa feedstock is shown in Fig. 11.

4.4. Characterisation of fuel pellets

Pellets resulting from each of the feedstocks were elaborated, sub jected to debinding and then densified under the conditions specified in Section 3 so as to assess their properties.

4.4.1. Analysis of fuel pellet microstructures

The resulting pellets were then cut up, coated and subjected to etch ing to reveal their microstructure. The results are shown in Fig. 12.

The five formulations Fa, Fb, Fc, Fd and Fe all share similar micro structures that are usually encountered for fuel pellets produced by standard powder metallurgy processes (pressing and sintering). The grain size varies between 7 and 15 μm in agreement with the specifica tions, with an intra and inter porosity distributed in a homogeneous manner.

The Ff formulation shows a very different microstructure with small grains about 5 μm in size and a very high porosity.

These microstructural changes can be due to a number of complex mechanisms, with the forming aid formulation having an impact on the final microstructure of the sintered pellet. Nonetheless, it is possible to distinguish two main mechanisms. The first is due to the type of forming aid added to the formulation. This potential chemical effect of the forming aids may especially explain the porosity change, with some polymers like PMMA playing a role of a pore forming material. The second mechanism is an indirect cause of the forming aid formula tion. Each formulation has a different viscosity due to the properties of the forming aid added to it. This means that the mixing torques (thus the stress applied to the powder) during the mixing stage are different. Deagglomeration will therefore occur differently, which means that the particle sizes and the polydispersity of the powder will thus be deter mined by the formulation used, with these two parameters influencing the grain sizes after the sintering stage. The carbon ratio after debinding can also influence the final microstructure.

The choice of formulation at the beginning of the process therefore makes it possible to control the final microstructure of the sintered pel lets. The contribution of each mechanism mentioned needs to be ex plored in depth to be able to accurately control the properties of the final pellet through the microstructure.

4.4.2. Analysis of the carbon ratio in the fuel pellets

The maximum residual carbon content specified for sintered pellets is 100 ppm.

To make sure that it is possible to come close to this specification, as says using a carbon analyser were performed on a pellet resulting from each of the formulations in question. The results of the 9 analyses per formed per pellet demonstrate the extremely good repeatability (Table 10).

The quantity of residual carbon is relatively similar regardless of the feedstock in question, give or take the measurement inaccuracies (±20 ppm). These results highlight the significant reduction in the car bon content of the pellets during the sintering stage. The quantity of

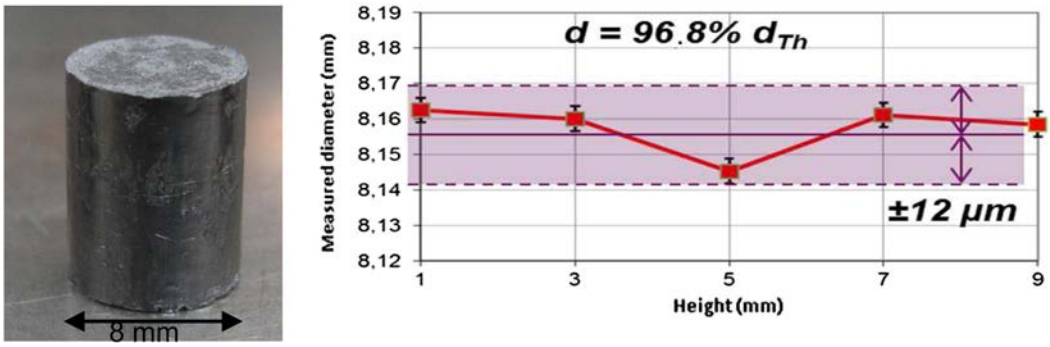

Fig. 13. Photograph of a fuel pellet fabricated by the injection moulding process; diameter profile of a fuel pellet.

carbon residue after debinding is between 2500 and 4000 ppm which reduces to somewhere between 100 and 150 ppm after sintering.

These figures are very close to the required specifications despite the debinding and densification conditions that were not optimised. Efforts therefore need to focus on optimising the debinding cycle to reduce the residual carbon content in the densified pellet to below the above mentioned specifications. Different solutions can be exploited: optimising the thermal cycle (in terms of the temperature plateaus and ramp ups), or changing the debinding technique (debinding by solvents, supercritical CO_2, etc.).

4.4.3. Fuel pellet metrology

The fuel specification on the pellet diameter is very strict: it must be ± 12 µm in relation to a specified diameter of 8.192 mm. With the actual fabrication process based on powder metallurgy, deformations of pellets occur during sintering because of density gradients in the green pellets after pressing, so that a mechanical grinding has to be performed on sintered pellets. This mechanical grinding step has a radiological impact and an economical cost. To prove that the injection moulding process is capable of directly producing net shape fuel pellets after sintering, pellets were fabricated with a feedstock initially loaded with 56 vol.% of UO_2 (use of the Fb formulation). The pellet with the best surface aspect has been selected for measurement of the diameter profile (surface defects are linked to the pressing tool). Fig. 13 shows the pellet and its diameter profile.

Using the injection moulding process therefore makes it possible to meet the geometric specifications without requiring a post sintering operation. Checking the pellet geometry is therefore a simple operation. Furthermore, hydrostatic density measurements indicate high figures around 96% of the theoretical density.

5. Conclusion

Six forming aid formulations have been assessed for powder injection moulding of uranium dioxide. Good rheological behaviours have been obtained for the six feedstocks loaded at 50 vol.%. No interaction has been noticed between polymers and UO_2.

Because the shear viscosity varies for the different forming aid formulations, deagglomeration of the powder varies too. So controlling the grain size characteristics of the powder may be possible through the choice of forming aid formulation as well as mixing conditions.

At the end, the forming aid formulation significantly influences the microstructure of sintered pellets, particularly in terms of grain size and porosity. More in depth analysis will therefore make it possible to control the final microstructure according to the forming aids used.

The mass of carbon residue resulting from the sintering stage an essential parameter when choosing a formulation was analysed; it falls below 150 ppm for all six formulations tested. The available margins for improving the debinding stage (mode, cycle) should make it possible to reduce this residue content even further.

Results obtained confirm that PIM process makes it possible to obtain net shape pellets directly after sintering without any post sintering operations.

According to the results of this study, the formulations to be recommended for the nuclear fuel application are those containing polystyrene. They provide good deagglomeration properties together with a low shear viscosity at the injection temperature. Moreover, they are theoretically resistant to radiolysis phenomena due to the benzene rings of the polystyrene.

These positive results have now to be consolidated with studies involving both UO_2 and PuO_2, especially to quantify radiolysis effects.

References

[1] Y. Guérin, J. Henckes, Conception et fabrication de combustibles à base d'uranium, Tech. Ing. BN3635 (2008).
[2] B. Mamen, J. Song, T. Barriere, J.-C. Gelin, Experimental and numerical analysis of the particle size effect on the densification behaviour of metal injection moulded tungsten parts during sintering, Powder Technol. 270 (2015) 230–243.
[3] O. Ozgun, H. Gulsoy, R. Yilmaz, F. Findik, Injection molding of nickel based 625 superalloy: sintering, heat treatment, microstructure and mechanical properties, J. Alloys Compd. 546 (2013) 192–207, http://dx.doi.org/10.1016/j.jallcom.2012.08.069.
[4] P. Thomas-Vielma, A. Cervera, B. Levenfeld, A. Varez, Production of alumina parts by powder injection molding with a binder system based on high density polyethylene, J. Eur. Ceram. Soc. 28 (2008) 763–771, http://dx.doi.org/10.1016/j.jeurceramsoc.2007.08.004.
[5] M. Belgacem, T. Barriere, J.-C. Gelin, Investigations on thermal debinding process for fine 316L stainless steel feedstocks and identification of kinetic parameters from coupling experiments and finite element simulations, Powder Technol. 235 (2013) 192–202, http://dx.doi.org/10.1016/j.powtec.2012.10.006.
[6] H. Ou, M. Sahli, J.-C. Gelin, T. Barrière, Experimental analysis and finite element simulation of the co-sintering of bi-material components, Powder Technol. 268 (2014) 269–278, http://dx.doi.org/10.1016/j.powtec.2014.08.023.
[7] M. Sahli, J.-C. Gelin, T. Barriere, Characterisation and replication of metallic microfluidic devices using three different powders processed by hot embossing, Powder Technol. 246 (2013) 284–302, http://dx.doi.org/10.1016/j.powtec.2013.05.026.
[8] R.M. German, R.G. Bose, Injection Molding of Metals and Ceramics, MPIF1997.
[9] B.C. Mutsuddy, R.G. Ford, Ceramic Injection Molding, Chapman & Hall, 1995.
[10] J. Bricout, J.C. Gelin, C. Ablitzer, P. Matheron, M. Brothier, Influence of powder characteristics on the behaviour of PIM feedstock, Chem. Eng. Res. Des. 91 (2013) 2484–2490, http://dx.doi.org/10.1016/j.cherd.2013.02.023.
[11] G. Rousseau, L. Desgranges, F. Charlot, N. Millot, J.C. Niepce, M. Pijolat, F. Valdivieso, G. Baldinozzi, J.F. Bérar, A detailed study of UO_2 to U_3O_8 oxidation phases and the associated rate-limiting steps, J. Nucl. Mater. 355 (2006) 10–20, http://dx.doi.org/10.1016/j.jnucmat.2006.03.015.
[12] L. Desgranges, H. Palancher, M. Gamaléri, J. Micha, V. Optasanu, L. Raceanu, T. Montesin, N. Creton, Influence of the U_3O_7 domain structure on cracking during the oxidation of UO_2, J. Nucl. Mater. 402 (2010) 167–172, http://dx.doi.org/10.1016/j.jnucmat.2010.05.014.
[13] R.J. McEachern, P. Taylor, A review of the oxidation of uranium dioxide at temperatures below 400 degrees C, J. Nucl. Mater. 254 (1998) 87–121, http://dx.doi.org/10.1016/S0022-3115(97)00343-7.
[14] D. Moinard, C. Rigollet, Procédés de frittage PIM, Tech. Ing. M3320 (2011).
[15] Th. Meyer, J. Keurentjes, Handbook of Polymer Reaction Engineering, Wiley-VCH, 2005.
[16] J. Bricout, Fabrication du combustible par injection: Etude de la formulation et du déliantage d'une pâte contenant des actinides(PhD) Université de Franche-Comté, France, 2012.
[17] M. Carrega, et al., Matériaux polymères, Dunod, 2005.
[18] I. Manas-Zloczower, Mixing and Compounding of Polymer, Hanser, 2009.